



Design and Experimental Study on a Flapping Wing Micro Air Vehicle

Yi Liu, Yanlai Zhang^(✉), and Jianghao Wu

School of Transportation Science and Engineering,
Beihang University, Beijing 100191, China
zhangyanlai@buaa.edu.cn

Abstract. Flapping Wing Micro Air Vehicles (FWMAVs), which are inspired by nature's flyers and mimic their flight, have numerous advantages compared with conventional fixed wing and rotating wing aircrafts at small scale and low Reynolds numbers, such as ability of hovering and anti-disturbance, high lift aerodynamic performance, good maneuverability. Due to the dimensional constraints and demands of compact design and low power consumption, suitable angles of attack and size of wings have to be tested to reach high aerodynamic efficiency. This paper presents results of experimental investigation of angle of attack (changed by a root deflection angle) and wingspan on the aerodynamics and power of a FWMAV. Based on the measured results, a quasi-steady model for lift and power estimation is suggested. The difference between the estimated and measured lifts and power is less than 10%, which reveals that the quasi-steady model is reasonable for a preliminary design. The results indicate that the wing with a root deflection angle around 15° shows the highest aerodynamic efficiency, and larger wings are preferred to reach a higher ratio of lift to power, implying that larger wing could give a higher lift under certain power input. Finally, we have obtained a best performance wing, which can generate about 40 g of lift at a power input of about 8 W when flapping at 22 Hz.

Keywords: Flapping Wing Micro Air Vehicles · Experimental measurement · Aerodynamics · Power consumption

1 Introduction

Micro air vehicles (MAVs) are a subclass of unmanned aerial vehicles (UAVs), limited to small size and light weight, with remotely piloted or autonomous operation. The bionic flapping-wing micro-aircraft has superior aerodynamic performance, manoeuvrability, and anti-disturbance ability compared with conventional fixed wing and rotating wing aircrafts at small scale and low Reynolds numbers [1]. Its small size, easy portability and strong concealment make it widely used in military investigations and civil counter-terrorism disaster relief. Therefore, research on flapping wing micro-aircraft is an important and meaningful event.

For these reasons, engineers have focused more on developing flapping-wing micro air vehicles (FWMAVs) [2–6] in recent years. A common FWMAV consists of a wing actuation mechanism, a pair of wings, a micro control system, a motor and a battery.

For flight, the FWMAV should be designed to generate a lift greater than its body weight. In order to optimize the FWMAV design, many studies have attempted to understand the effect of different parameters like wing area, angle of attack and flapping amplitude on the aerodynamic force generation and power consumption of flapping wing using CFD and quasi-steady methods [8–11], and results show that they all have a significant effect on aerodynamic performance. However, for the actual design of a FWMAV, due to the fact that the wings will inevitably have deformation during flapping and inaccurate assembly results in gaps between different mechanisms, it is difficult to accurately analyze the lift and power consumption of the system by numerical simulations, so it is necessary to use experimental measurement to further verify the simulation results.

The objective of this paper is to analyze the aerodynamic performance of a FWMAV by combining experimental and numerical method. We have learned from the previous works [5, 7] on the design of the mechanism and successfully used 3D printing technology to design and manufacture a flapping mechanism that can work at a high flapping frequency and operate for a long time. Subsequently, the aerodynamic lift and power consumption of the wing at different flapping angles of attack are investigated by experimental measurements. By changing the root deflection angle of wing to change angles of attack [15], the time course of wing deformation and wing flapping angles and angles of attack were extracted from images captured by a high speed camera. We found that different angles of attack and flapping frequencies will affect the wing flapping amplitude significantly. In addition, we used the quasi-steady aerodynamic model [9, 11] to estimate the lift and power consumption of those wings and also used a load cell to measure the corresponding lift and power and a vacuum chamber to measure inertial power. Then, the results of estimation and experimental measurement are compared, showing that the quasi-steady model is proper for initial design when considering real kinematics and deformations. Finally, using the quasi-steady model, we evaluated the lift and power consumption of different wings with different wingspans and analyzed the results applying to the design of FWMAV.

2 Flapping-Wing System and Experimental Method

2.1 Flapping Mechanism and Wing

The flapping mechanism, as shown in Fig. 1, is learned from Ref. [7]. It adopts a single-crank double rocker movement form, and the components are made of nylon material by 3D printing. With moderate density, high strength and stiffness, nylon material is suitable for processing flapping mechanism. The parts are connected by light aluminum rivets and the design flapping amplitude is 130° . During flapping, the maximum flapping amplitude can reach about 170° due to assembly gap and the structural elastic deformation. This design can also change the flapping amplitude easily by altering the length of the crank.

The design of the wing adopts a method of torsional deformation along the length of the wing. This design method is widely used in FWMAVs like Nano hummingbird and some studies [12–14] have shown that this wing design method exhibits better

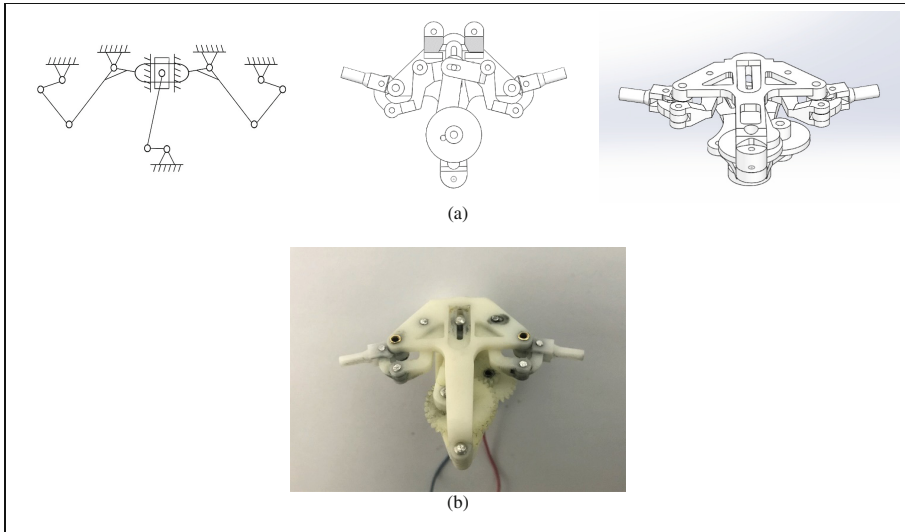


Fig. 1. (a) 3D design drawing of flapping mechanism (b) fabrication of the flapping mechanism

aerodynamic performance than the flat rigid wing and also has some advantages, such as easy processing and less vibration. As shown in Fig. 2, wings are manufactured of carbon fiber rods and PET. The carbon fiber rod with a diameter of 1 mm was selected as the leading edge of the wing, and the carbon rod with a diameter of 0.5 mm was used on surface to maintain the shape of the wing when flapping. The wing film was a PET film with a thickness of 0.02 mm. The membrane at wing root is bonded to the root carbon rod attached to the mechanism. When adjusting the angle of attack, the deflection angle of the membrane at wing root can be changed and the corresponding wing root bonding line is adhered to the fixed root carbon fiber (as shown in Fig. 2(c)). When the deflection angle is small, the wing membrane is tight and there will be a large angle of attack. On the contrary, when the deflection angle is large, the wing membrane will become slacker and the angle of attack will become smaller.

2.2 Measurement of Wing Kinematics, Lift and Power

In experiments, we need to obtain the flapping amplitude and angle of attack variation in a flapping period. A high-speed camera (MotionXtra HG-LE) is used to capture the wing while it is flapping at about 20 Hz – 30 Hz. Figure 3(a) shows the experimental platform used in the present study. The camera is horizontally placed and a mirror is tilted by 45° to horizontal to get a top view of the flapping-wing system. The filming frequency is 2500 fps which can capture the wing motion clearly. Figure 3(b) shows the captured images. Overlapping the start and end images in a stroke, we can measure the flapping amplitude. The angles of attack at different wing spanwise position can be measured by calculating the cosine of angle between the wing chord and its projection.

The study of the aerodynamic characteristics of the wing requires a relatively accurate measurement of lift. The load cell selected for lift force measurement is a

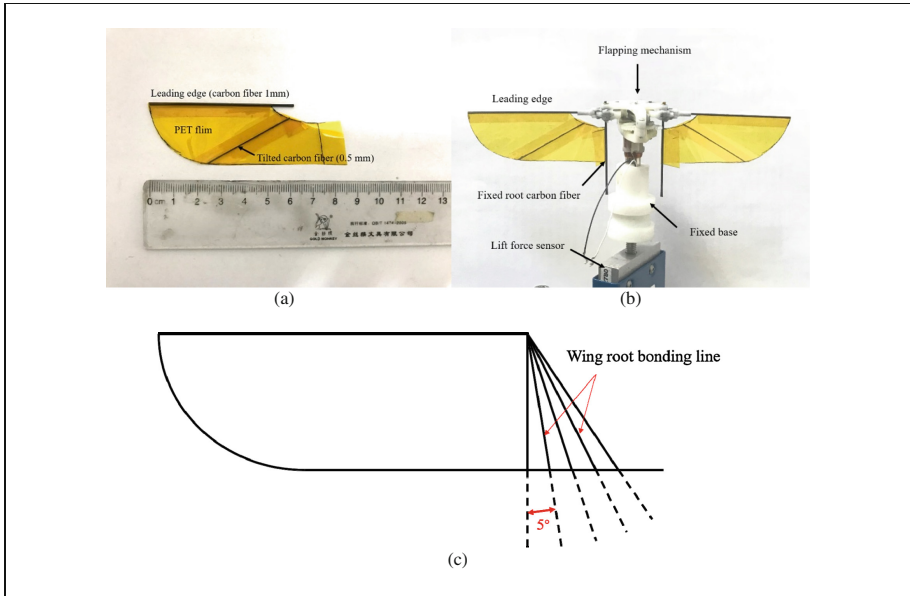


Fig. 2. (a) Experimental wing and (b) installation method (c) change the deflection angle to adjust the flapping angle

SMT1 sensor of American Interface Corporation. The maximum standard load is 10 N (1000 g) and the accuracy is 0.0001 N, the instantaneous safety overload can reach 10 times standard load. In the experiment, a fixed base with the flapping mechanism is vertically fixed on the load cell.

During force measurement, the power required by the FWMAV to flap the wings was recorded synchronously, similar to Ref. [15]. During flapping motion, the power input (P_{in}) was spent to produce an aerodynamic force (power of aerodynamic, P_{AE}), and a back and forth motion of the flapping mechanism (power of flapping mechanism, P_M), and to overcome the inertia of the wings during the flapping motion (wing inertia power, P_I). And some proportion of the power input is lost as the Joule heating loss in motor (power loss, P_{Loss}). Thus, the power input (P_{in}) can be broken down as follows:

$$P_{in} = P_{Loss} + P_M + P_{AE} + P_I \quad (1.1)$$

In order to obtain the mechanism power consumption (P_M) of the flapping mechanism, we uninstalled the wings and let the mechanism flap only, then recorded the voltage and current between the two ends of the motor. The wing inertia power (P_I) was measured in a vacuum chamber, by subtracting the corresponding mechanism power (P_M) from the total input, as shown in Fig. 4.

Finally, the flapping mechanism tested in the vacuum chamber was placed in a normal pressure environment and fixed on the lift sensor to perform the same experiment. The lift was measured synchronously. From this step-by-step experiment, we can measure the power consumption of each part of the flapping MAVs.

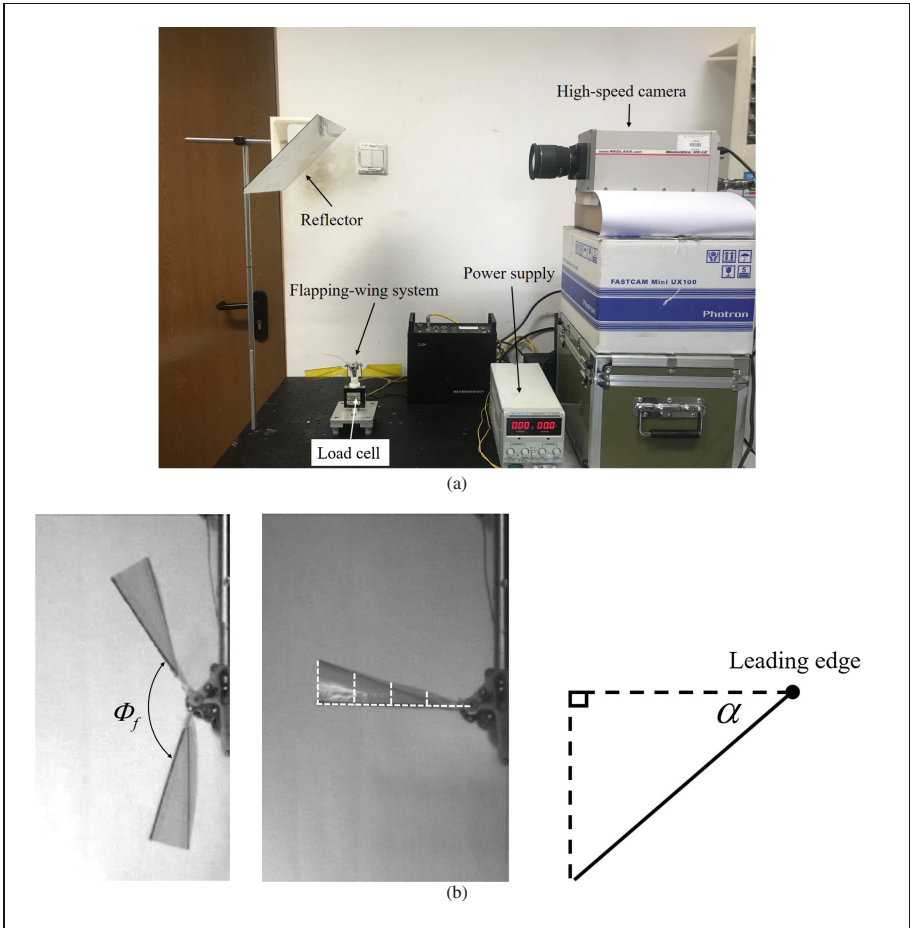


Fig. 3. (a) High-speed camera platform (b) flapping amplitude and flapping angle of attack obtained from high-speed camera images

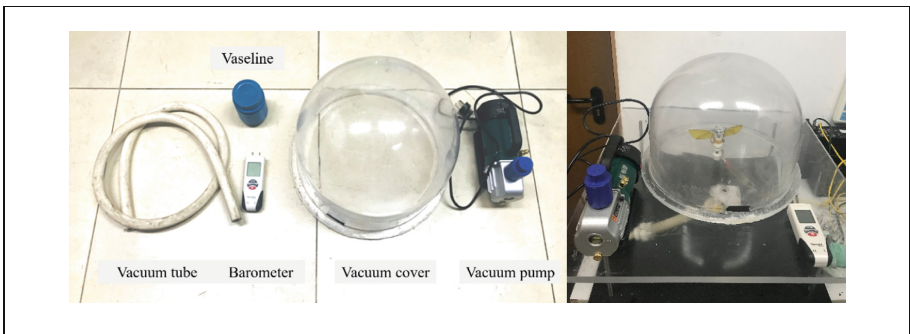


Fig. 4. Vacuum test platform

3 Results and Discussion

3.1 Effect of Angle of Attack on Aerodynamic Characteristics

From the aforementioned experimental steps of power consumption measurement, the mechanical power consumption of the mechanism was measured at several flapping frequencies (as shown in Fig. 5). And then we used an exponential function (Eq. 1.2) to fit these points. In the next experimental study, the fitting equation can be used to estimate the power consumption of the flapping mechanism.

$$P_M = 1.371 \times 10^{-4} f^{2.25} \quad (1.2)$$

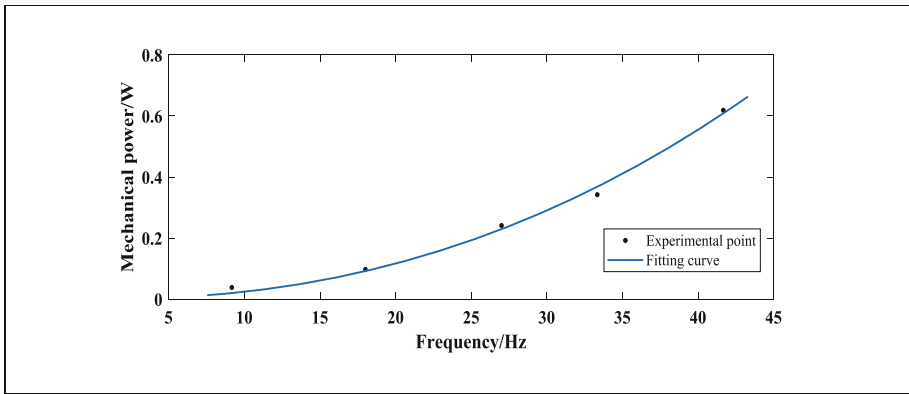


Fig. 5. Mechanical power consumption at different flapping frequency

As shown in Fig. 2(c), the wing angles of attack can be adjusted through changing the root deflection angle. In the present paper, we chose a wing with a wingspan of 8 cm (aspect ratio $AR = 3$) and measurements of five angles of attack were conducted by varying the root deflection angles (0° , 5° , 10° , 15° , and 20°). The larger the deflection angle is, the smaller the angle of attack is. The high-speed camera captured the angle of attack of the wing tip and the flapping angle of the wing (Fig. 6(a)). It can be seen that different root deflection angles indeed result in different angles of attack, and the time history of wing flapping angle in a flapping period agrees well with a sinusoidal function as designed. There exists a peak/valley at the end/start of a stroke, due to the fact that the inertia of the wing drives the wing to pitch continuously, resulting in a smaller angle of attack. In the next moment, the angle of attack of the wing with a larger root deflection angle will increase, this is because in the start of flapping, the flapping speed is slow, and the lift of the wing is small, as a result, the weight of the wing itself drives the wing to deflect downwards at the speed. After the lift increases, the wing will maintain a certain angle of attack.

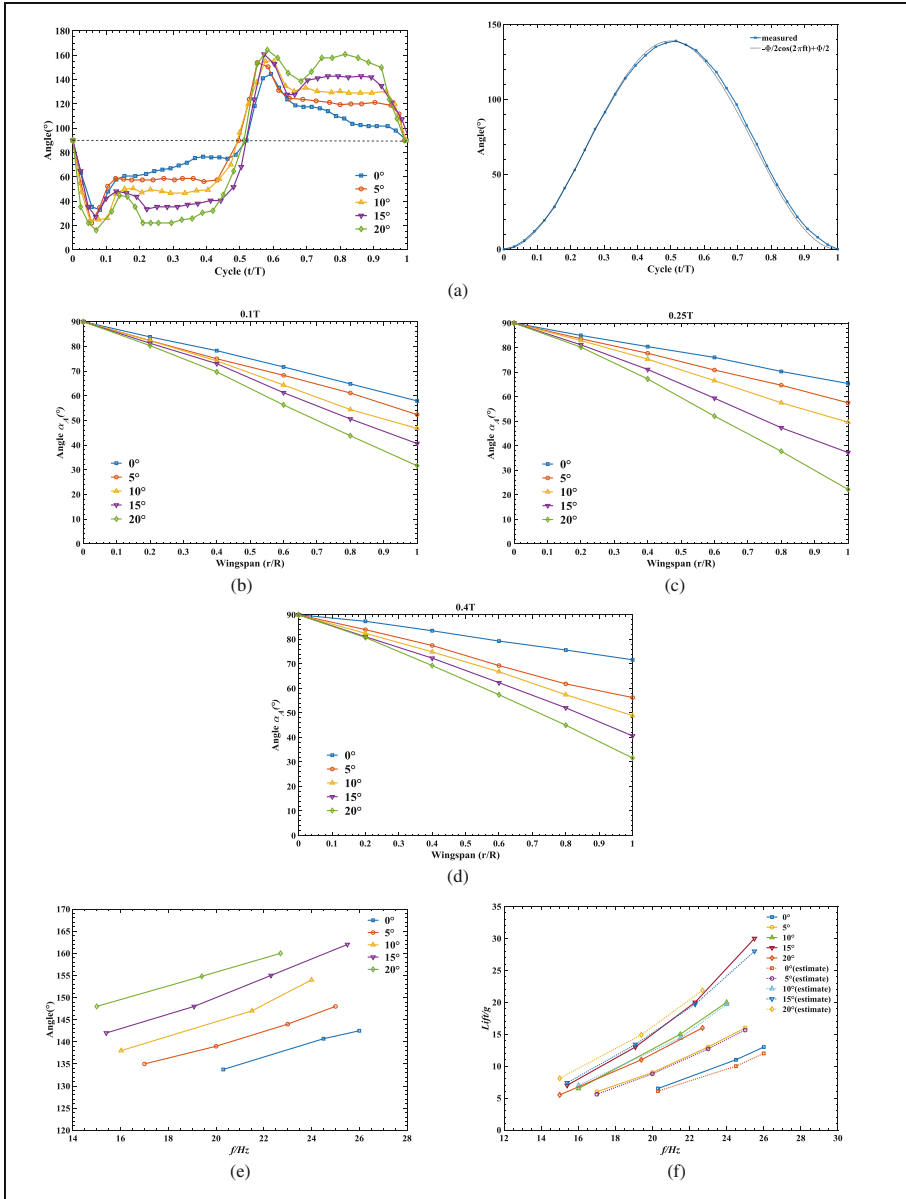


Fig. 6. (a) The angle of attack of the wing tip and the flapping angle of the wing in a flapping cycle. (b) (c) (d) average geometric angle of attack during translational stage ($t/T = 0.1, 0.25$ and 0.4) along the wingspan in one flapping cycle. (e) the flapping amplitude varies with flapping frequency and angle of attack. (f) the measured lift and estimate lift using quasi-steady theory.

From Fig. 6(b) (c) (d), we draw the average geometric angle of attack during translational stage ($t/T = 0.1, 0.25$ and 0.4) along the wingspan in one flapping cycle, they respectively correspond to the end of the wing flipping, the maximum flapping speed moment and the start of the wing flipping. We can see the angle of attack of different sections along the wingspan varies linearly. Therefore, the assumption of linear torsion along wing spanwise could be acceptable, which is used in the following quasi-steady aerodynamic model.

In experiments, we found that the flapping amplitude varies with the angle of attack and the flapping frequency. The design flapping amplitude of the flapping mechanism is 130° , Fig. 6(e) shows that the flapping amplitude increase as the flapping frequency increases. It is found that the inertia force of the wing increases with the flapping frequency of, this will cause the deformation of the mechanism and the wing to increase due to the slight elastic deformation of the mechanism material and the wing itself. Therefore, the increase of the flapping frequency will result in a larger flapping amplitude. In addition, it can be seen from Fig. 6(e) that at the same flapping frequency, the flapping amplitude also increases with the wing root deflection angle. This is because if the wing's angle of attack is smaller, when the wing flips, the wing will have a greater flipping inertia force, which will increase the elastic deformation of the mechanism and the wing as well. So different flapping angles of attack will also cause slight differences in flapping amplitude. Therefore, for the real FWMAV design, these influencing factors need to be taken into account.

The input parameters of the quasi-steady model can be modified by the actual motion parameter. Figure 6(f) shows the measured lift and estimate lift using quasi-steady theory, we can see that when the root deflection angle is changed from 0° to 15° , the lift force increases at the same flapping frequency, and the experimental results are in good agreement with the estimation results. The largest relative error is 7%. When the root deflection angle is 20° , the experimental results are very different from the estimation results, and the experimental results are much smaller. From the flapping images, this is because when the root bonding angle is 20° , the wing of the experimental model is too loose, and the wing lift cannot be conducted at the root, causing the flapping lift to be smaller than the theoretical estimation.

In the study of the angle of attack on aerodynamic characteristics, we are more concerned with the aerodynamic efficiency of different angles of attack, that is, the relationship between the aerodynamic power consumption (P_{AE}) and the lift force. Therefore, we measured the inertial power (P_I) consumption of the flapping motion, so that the aerodynamic power consumption under different flapping angles of attack can be obtained, and then the aerodynamic efficiency at different angles of attack can be analyzed. Figure 7(a) shows the measured inertial power of the wingspan. Furthermore, we have estimated the inertial power consumption based on the parameters and quality of the wing, and found that the trend of the test results is very close to the trend of the estimation results, and the actual measurement results are slightly larger than the estimation results by about 10%. Because the air pressure in the test vacuum environment is 5 kPa and it is difficult to reduce the vacuum air pressure furthermore, the wing still has a certain aerodynamic power consumption in the flapping motion, so the

inertial power of the test will be larger than the actual inertial power. After measuring the inertial power consumption (P_I), the aerodynamic power consumption (P_{AE}) of the wing flapping is further obtained (as shown in Fig. 7(b)), and we plot the lift versus the aerodynamic power consumption of the wing in Fig. 7(c).

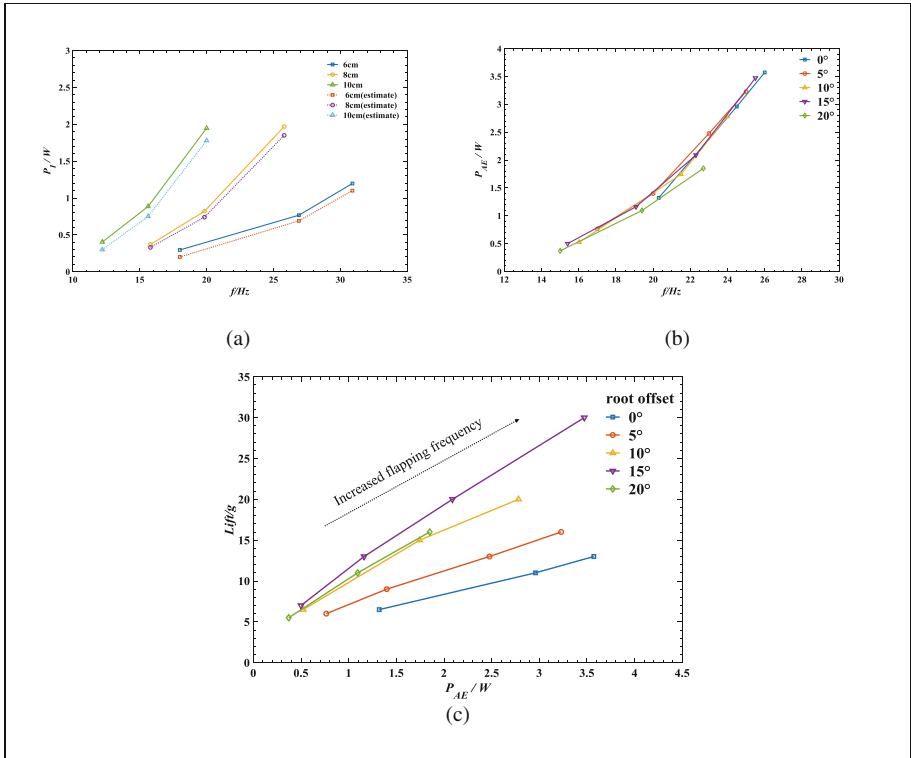


Fig. 7. (a) measured and estimated inertial power consumption. (b) aerodynamic efficiency at different flapping angles of attack. (c) lift versus the aerodynamic power consumption of the wing

Figure 7(b) shows that wings with different flapping angles of attack at the same flapping frequency consume almost the same aerodynamic power. As mentioned before, the angle of attack will also affect the flipping amplitude, so the combined effect of the two results in almost the same aerodynamic power consumption for different flapping angles of attack. Figure 7(c) shows that the optimal aerodynamic efficiency angle of attack is the wing whose wing root deflection angle is 15°. When the wing root deflection angle is larger, the wing lift force will decrease, so the aerodynamic efficiency will be reduced. When the wing root deflection angle is 15°, the angle of attack of the wing tip is about 35°, and the second moment of the wing has an angle of attack of about 55° which is similar to the result in [15]. Therefore, in the design of the angle of attack for the FWMAVs, the deflection of the wing root around 15° is a better choice, which has the highest aerodynamic efficiency.

Table 1 shows the comparison between the measured aerodynamic power at different angles of attack and the quasi-steady theory estimated power consumption. The result shows that the maximum relative difference is within 10%, which can be used to estimate the flapping aerodynamic power consumption effectively.

Table 1. Comparison of estimated and measured aerodynamic power consumption (P_{AE})

	Frequency (Hz)	Measured P_{AE} (W)	Estimate P_{AE} (W)	Difference (%)
8 cm 0°	20.3	1.32	1.3	1.5
	24.5	2.96	2.7	8.8
	26	3.57	3.36	5.8
8 cm 5°	17	0.76	0.73	4
	20	1.39	1.3	6.5
	25	3.22	3.1	3.7
8 cm 10°	16	0.52	0.56	7.7
	21.5	1.74	1.67	4
	24	2.78	2.67	4
8 cm 15°	15.4	0.5	0.5	0.1
	19.1	1.16	1.08	7
	25.5	3.47	3.4	2
8 cm 20°	15	0.37	0.4	-8
	19.4	1.1	1	9
	22.7	1.84	1.77	3.8

3.2 Effect of Wingspan on Aerodynamic Characteristics

Another research focus is the effect of wing area on aerodynamic characteristics. The choice of wing area has a significant effect on flapping wing power efficiency. A larger area wing will provide higher aerodynamic lift, but it will also require more aerodynamic and inertial power. Therefore, it is worth studying what wing area can provide higher power efficiency. In the previous section, we verified that the quasi-steady theory model can well estimate the aerodynamic lift, aerodynamic power consumption and inertial power consumption. So, in this section, in order to avoid a lot of experimental work, we first use the quasi-steady model to analyze the effect of wing area on aerodynamic characteristics, then we experimentally validate the wing with the highest power efficiency.

From the conclusion of the previous section, the deflection of the wing root around 15° has a higher aerodynamic efficiency, so we fixed the wing root deflection angle at 15° in this section, the angle of attack at the second moment of the wing is about 55°. The aspect ratio (AR) of the wing is fixed at 3, which has been proved to have a higher aerodynamic efficiency [16]. As a result, we chose the wingspan as the parameter of the study instead.

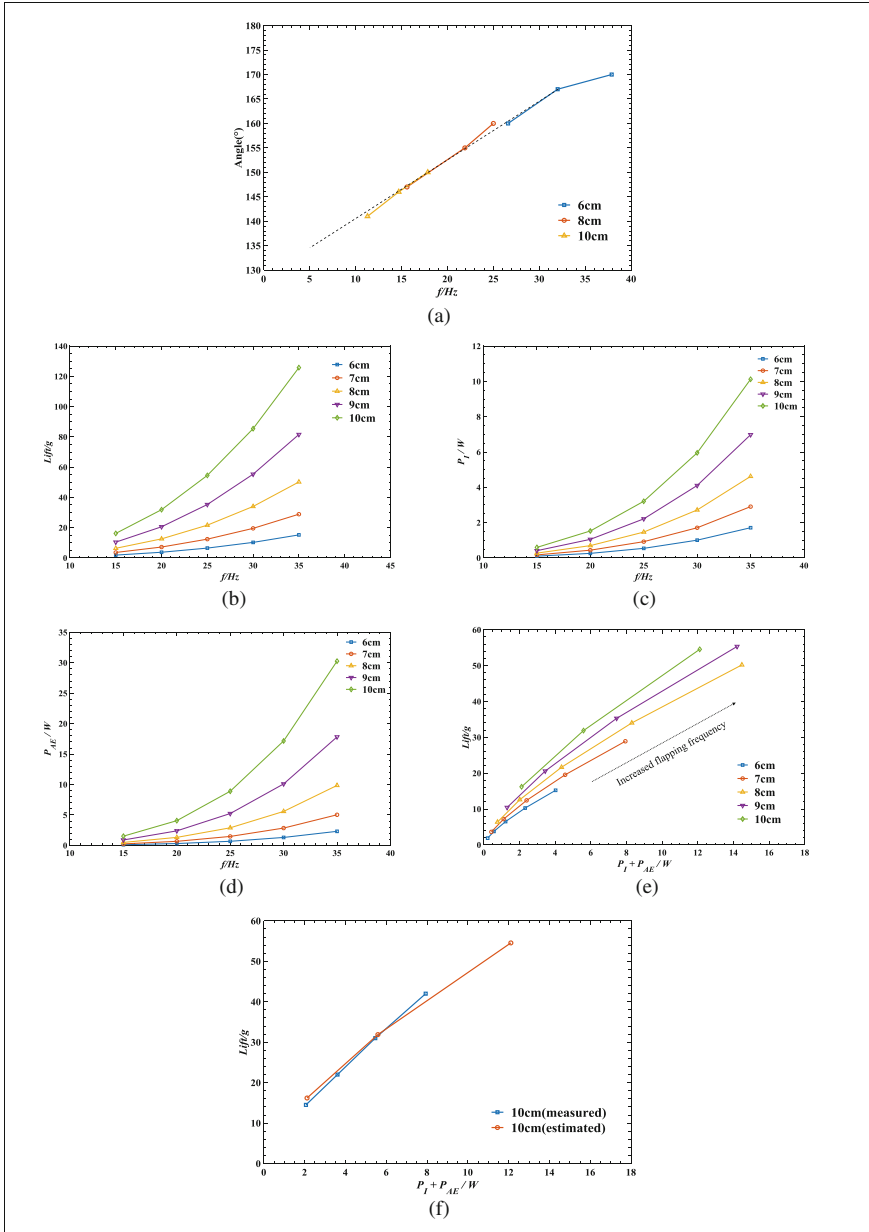


Fig. 8. (a) Flapping amplitude varies with frequency. (b) (c) (d) Lift, inertial power consumption, and aerodynamic power consumption of the wing. (e) Lift versus total power consumption of different wingspans. (f) Measured and estimated results of the 10 cm wing.

Since the estimation model requires the accurate flapping amplitude of FWMAV, the previous experiment found that the flapping amplitude increases with the flapping frequency. So we experimentally measured the flapping amplitude of different wingspans at the same root deflection angle, as shown in Fig. 8(a). It can be found that when the flapping frequency is within 35 Hz, the flapping amplitude changes substantially linearly with the flapping frequency. When the frequency is higher than 35 Hz, due to the constraints of the mechanism, it will basically reach the limit of the flapping amplitude about 170° . Since the FWMAV operation flapping frequency is basically within 35 Hz, a linear function can be used for fitting and can be written as follows:

$$\Phi_f = \frac{10}{7}f + 130 \quad (1.3)$$

We studied the wingspans from 6 cm to 10 cm and estimated the flapping lift, aerodynamic power consumption, and inertial power consumption of the wing at different frequencies, as shown in Fig. 8(b) (c) (d), it can be seen that the lift is basically proportional to the square of the flapping frequency, and the power consumption is proportional to the third power of the flapping frequency. The wings with larger wingspan can produce higher lift but at the same time consume more inertial power and aerodynamic power. From the estimation results, we can then obtain the Fig. 8(e), the relationship between the total power consumption ($P_{AE} + P_I$) and the lift. It shows that the wing with larger wingspan can produce higher lift with the same total power consumption. The 10 cm wing has the highest power efficiency.

In order to verify the accuracy of the estimation results, we performed an experimental measurement on the 10 cm wing. The root deflection angle is 15° and the angle of attack at the second moment is still about 55° . The comparison between the measurement results and the estimation results is shown in Fig. 8(f). We can see that the experimental results are in good agreement with the estimation results. When generating a 40 g lift, it takes about 8 W of total power and the flapping frequency is 22 Hz.

4 Conclusion

This paper presented the results of experimental study of angle of attack and wingspan for a FWMAV. Experiments were carried out to measure the lift and aerodynamic power consumption of different flapping angles of attack. The inertial power consumption of wings with different wingspans were also measured in the vacuum test platform. The paper also uses the quasi-steady model to estimate the lift and aerodynamic power consumption and it is found that the experimental results are in good agreement with the estimation results. Thus, in the design of the FWMAV, the quasi-steady method can be well used for rapid engineering estimation.

The results of the paper show that when the wing root deflection is about 15° , the wing presents the highest the aerodynamic efficiency, which is a better design for the FWMAV. For wings with different wingspans, larger wing requires less power when producing the same lift. The larger the wing is, the higher the power efficiency is.

Therefore, through experiments and estimations, we have obtained a better wing design for a FWMAV, which has a 15° wing root deflection angle and 10 cm wingspan, and it can generate about 40 g of lift at a power input of about 8 W when flapping at 22 Hz.

Acknowledgements. This research was primarily supported by the National Natural Science Foundation of China (NSFC, Grant No. 11672022).

References

1. Muijres FT, Elzinga MJ, Melis JM, Dickinson MH (2014) Flies evade looming targets by executing rapid visually directed banked turns. *Science* 344:172–177
2. Keennon M T, Klingebiel K, Won H, Andriukov A (2012) Development of the nano hummingbird: a tailless flapping wing micro air vehicle. In: *Proceedings of 50th AIAA Aerospace Sciences Meeting* (Nashville, Tennessee)
3. Ma KY, Chirarattananon P, Fuller SB, Wood RJ (2013) Controlled flight of a biologically inspired insect-scale robot. *Science* 340:603
4. Phan HV, Nguyen QV, Truong QT, Truong VT, Park HC, Byun DY, Goo NS, Kim MJ (2012) Stable vertical takeoff of an insect-mimicking flapping-wing system without guide implementing inherent pitching stability. *J Bionic Eng*
5. Phan HV, Kang TS, Park HC (2017) Design and stable flight of a 21 g insect-like tailless flapping wing micro air vehicle with angular rates feedback control. *Bioinspir Biomim* 12:036006
6. Wood RJ (2008) The first takeoff of a biologically inspired at scale robotic insect. *IEEE Trans Robot* 24:1–7
7. Karásek M, Hua A, Nan Y, Lalami M, Preumont A (2014) Pitch and roll control mechanism for a hovering flapping wing MAV. *Int. J Micro Air Veh* 6:253–264
8. Ansari SA, Knowles K, Zbikowski R (2008) Insect-like flapping wings in the hover part 2: effect of wing geometry. *J Aircr* 45:1976–1990
9. Truong QT, Nguyen QV, Truong VT, Park HC, Byun DY, Goo NS (2011) A modified blade element theory for estimation of forces generated by a beetle-mimicking flapping wing system. *Bioinspir Biomim* 6:036008
10. Phan HV, Truong QT, Park HC (2017) An experimental comparative study of the efficiency of twisted and flat flapping wings during hovering flight. *Bioinspir Biomim* 12:036009
11. Lee YJ, Lua KB, Lim TT et al (2016) A quasi-steady aerodynamic model for flapping flight with improved adaptability. *Bioinspi Biomim* 11(3):036005
12. Phan HV, Truong QT, Au TK, Park HC (2016) Optimal flapping wing for maximum vertical aerodynamic force in hover: twisted or flat? *Bioinspir Biomim* 11(4):046007
13. Zheng L, Hedrick TL, Mittal R (2013) Time-varying wingtwist improves aerodynamic efficiency of forward flight in butterflies. *PLoS ONE* 8:e53060
14. Du G, Sun M (2010) Effects of wing deformation on aerodynamic forces in hovering hoverflies. *J Exp Biol* 213: 2273–83
15. Nguyen TA, Phan HV, Au TKL, Park HC (2016) Experimental study on thrust and power of flapping-wing system based on rack-pinion mechanism. *Bioinspir Biomim* 11:046001
16. Du G, Sun M (2010) Effects of wing deformation on aerodynamic forces in hovering hoverflies. *J Exp Biol* 213: 2273–2283